Ab initio x-ray absorption study of Mn K-edge XANES spectra in Mn_3MC (M = Sn, Zn and Ga) compounds

2007 J. Phys.: Condens. Matter 19 216214

(http://iopscience.iop.org/0953-8984/19/21/216214)

IOP PUBLISHING JOURNAL OF PHYSICS: CONDENSED MATTER

J. Phys.: Condens. Matter **19** (2007) 216214 (9pp) doi:10.1088/0953-8984/19/21/216214

Ab initio x-ray absorption study of Mn K-edge XANES spectra in Mn_3MC (M = Sn, Zn and Ga) compounds

J Chaboy[1], **H Maruyama**[2] **and N Kawamura**[3]

[1] Instituto de Ciencia de Materiales de Aragón, CSIC-Universidad de Zaragoza, 50009 Zaragoza, Spain
[2] Graduate School of Science, Hiroshima University, 1-3-1 Kagamiyama, Higashi-Hiroshima 739-8526, Japan
[3] SPring-8/JASRI, 1-1-1 Kouto, Sayo, Hyogo 679-5198, Japan

Received 27 November 2006, in final form 27 March 2007
Published 1 May 2007
Online at stacks.iop.org/JPhysCM/19/216214

Abstract

This work reports a theoretical x-ray absorption near-edge structure (XANES) spectroscopy study at the Mn K-edge in several Mn_3MC (M = Sn, Zn and Ga) compounds. Comparison of the experimental Mn K-edge XANES spectra and theoretical computations based on multiple scattering theory shows that standard single-channel calculations are not able to reproduce the experimental spectra. The comparison between experimental data and *ab initio* computations indicates the need to include the charge transfer and hybridization between the absorbing Mn atom and the two nearest neighbour C atoms.

(Some figures in this article are in colour only in the electronic version)

1. Introduction

The ternary carbide phase Mn_3MC (M = Sn, Zn and Ga) compounds have attracted great attention in recent years due to their large variety of magnetic orderings and structural transformations [1, 2]. These compounds exhibit the antiperovskite structure, having an analogy to that of the perovskite oxides. However, their physical properties are very different and the Mn_3MC compounds show intriguing magnetic structures that have been studied intensively [1–4].

Mn_3GaC has an antiferromagnetic (AFM) phase in the ground state [3]. Upon heating, it shows a first-order transition to the ferromagnetic (FM) phase at the transition temperature $T_t \sim 160$ K through a small region of the intermediate state where both the AFM and FM components are present [5, 6]. The Curie temperature of Mn_3GaC is $T_C = 250$ K. The magnetic behaviour strongly depends on the C stoichiometry. Indeed, the spin configuration and the magnetic structure vary in a complicated way by electron or hole doping in the Mn antiperovskite system [2].

In the case of Mn_3GaC the AFM region disappears with a small deficit of C (4%) [1]. For effectively one-hole-doped Mn_3ZnC the spin configuration becomes noncollinear with a tetragonal magnetic structure, and the AFM and FM phases coexist in the ground state [4]. By

contrast, for effectively one-electron doped Mn_3SnC the spin configuration is also noncollinear up to $T_C = 290$ K; unlike the above compounds, Mn_3SnC does not have a stable FM phase. In these three compounds the results of neutron diffraction show that the magnetic moments of Mn atoms are much smaller than those observed for the other manganese intermetallic compounds ($\sim 4\ \mu_B$). This result can be interpreted as reflecting the strong itinerant character of the Mn-3d electrons in these compounds.

Knowledge of the electronic structure of these compounds is crucial to get a complete understanding of their magnetic and structural properties. Band structure calculations have suggested that the density-of-states (DOS) shows a sharp resonance near E_F [7–9]. The fact that the Fermi level lies close to the sharp peak of the DOS implies a strong dependence of the magnetic and structural properties of these systems upon the modification of the effective number of conduction electrons. Moreover, these calculations have shown that there exists a strong hybridization between Mn 3d and C 2p states. Due to this hybridization, the bandwidth of Mn 3d states becomes wide so that the system behaves as an itinerant–electron system [8].

An experimental insight into the electronic structure of these systems can be obtained by means of spectroscopic methods. Uemoto *et al* have reported a combined x-ray absorption spectroscopy (XAS) and x-ray magnetic circular dichroism (XMCD) study performed at the Mn K-edge in Mn_3MC (M = Sn, Zn and Ga) compounds [10]. The differences observed in the XMCD spectra were tentatively assigned to the charge transfer from the M metal towards Mn. Later, Takahashi and Igarashi performed *ab initio* computations of both the XMCD and XAS spectra of Mn_3GaC [11]. Despite band structure calculations pointing out the importance of C atoms in the electronic structure of these systems, none of these works discussed the role of the hybridization between Mn 3d and C 2p states in the absorption spectra.

In this work, we present a systematic study of the Mn K-edge x-ray absorption near-edge structure (XANES) spectra in several manganese carbide Mn_3MC (M = Sn, Zn and Ga) compounds. We have performed detailed *ab initio* computations of the absorption spectra within the multiple-scattering framework. Our aim was to determine the influence of the nature of the Mn–C bond, metallic or ionic-like, on the XANES spectra recorded at the Mn K-edge. Consequently, special attention has been paid to establishing the improvements obtained by using self-consistent-field (SCF) methods to describe the final state potential and the different treatments of the exchange–correlation part. Our results point out the key role of the hybridization between Mn atoms and their next-neighbour carbon atoms in determining the shape of the whole XAS spectra. Our results support the previous band structure calculation, suggesting the importance of C atoms in determining the magnetic properties of the Mn_3MC systems through the Mn 3d and C 2p hybridization.

2. Computational methods

Computation of the XANES spectra was carried out using the multiple-scattering code CONTINUUM [12] based on the one-electron full-multiple-scattering theory [13, 14]. A complete discussion of the procedure can be found in [15] and [16].

The potential for the different atomic clusters was approximated by a set of spherically averaged muffin-tin (MT) potentials built by following the standard Mattheis prescription [17]. The muffin-tin radii were determined following Norman's criterion and by imposing an overlapping factor of 10% [18]. The Coulomb part of each atomic potential was generated using charge densities for neutral atoms obtained from the tabulated atomic wave functions by Clementi and Roetti [19]. The atomic orbitals were chosen to be neutral for the ground state potential, whereas different choices were used to build the final state potential: (i) screened and relaxed $Z + 1$ approximation [20] and (ii) self-consistent field potential (SCF). Regarding

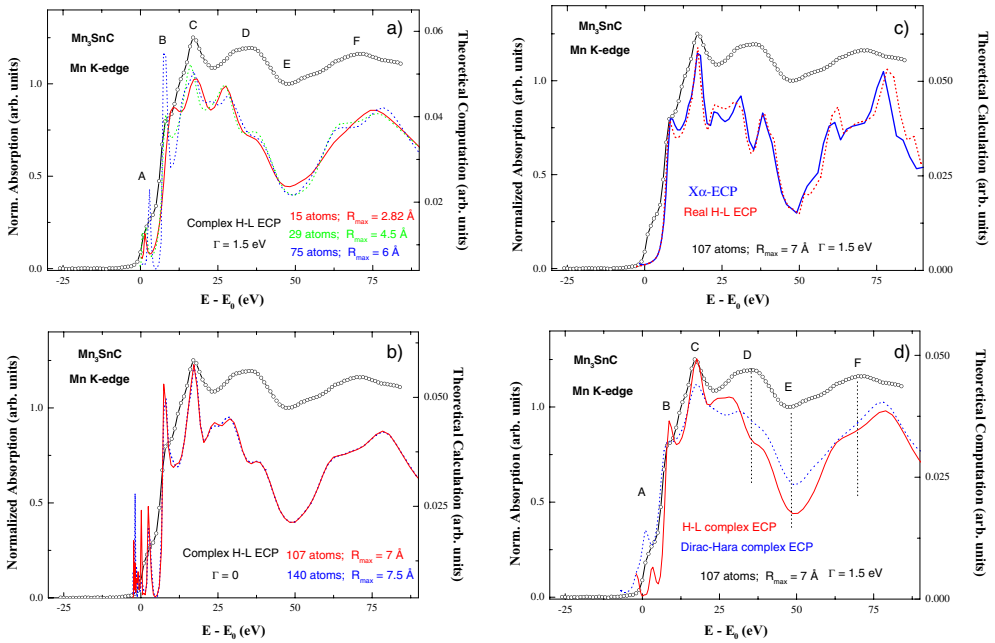

Figure 1. (a) Comparison of the experimental XANES spectrum at the Mn K-edge in Mn_3SnC (O) and the results of the calculations performed by using the HL potential and progressively adding neighbouring shells around the absorbing Mn covering up to: 2.82 Å (red, solid line), 4.5 Å (green, dotted line) and 6 Å (blue, dashed line). (b) Same (a) for cluster sizes of 7 Å (red, solid line) and 7.5 Å (blue, dots). (c) Results of the computations performed for a 7 Å cluster and by using X_α (blue, solid) and the real part of the HL potential (red dots). (d) Same as (c) for both complex HL (red, solid) and DH (blue, dots) potentials.

the exchange and correlation parts of the final state potential we have used three different types: X_α, the energy-dependent Hedin–Lundqvist (HL) complex potential and the energy-dependent Dirac–Hara (DH) exchange potential. The calculated theoretical spectra have been further convoluted with a Lorentzian shape function to account for the core-hole lifetime ($\Gamma = 1.5$ eV) [21].

The results of the calculations have been compared to the experimental XAS spectra reported by Uemoto *et al* [10].

3. Results and discussion

Systematic *ab initio* calculation of the Mn K-edge XANES spectrum was performed for Mn_3SnC, Mn_3ZnC and Mn_3GaC. This series of compounds have the antiperovskite Mn_3MC cubic structure. The antiperovskite structure locates Mn atoms at the face centres, transition-metal element M (=Zn, Ga, Sn) atoms at the octahedral corners, and C atoms at the body centre. The nearest-neighbouring environment of Mn in Mn_3MC corresponds to two C atoms located at $R_{\mathrm{Mn-C}} = 1.99$, 1.965 and 1.94 Å for M = Sn, Zn and Ga, respectively [2, 3]. The second coordination shell is formed by six Mn atoms and six M atoms located at the same interatomic distance $R_{\mathrm{Mn-M}} = 2.82$, 2.78 and 2.75 Å for M = Sn, Zn and Ga, respectively.

First calculations were done for Mn_3SnC. As shown in figure 1, the experimental XANES spectrum shows several absorption features: (i) a shoulder-like structure, A, at the rising edge;

(ii) a step-like feature, B, at $\Delta E \sim 8$ eV above the edge; (iii) the main absorption line C at ∼17 eV; (iv) a broad resonance, D, at ∼35 eV; and finally (v) a deep minimum E at ∼48 eV above the edge. Initially, we have determined the minimum size of the cluster needed to reproduce all the structures present in the experimental XANES spectra. To this end, we have performed different calculations, progressively increasing the number of atoms in the built-up cluster. Figure 1 reports the result of the computations obtained by using a cluster of 15 atoms covering a range of ∼2.9 Å around the absorbing Mn. The computation for this cluster includes all the scattering (single and multiple) paths involving the two C atoms of the first coordination shell and the 12 atoms (six Mn and six Sn) located at the same interatomic distance with respect to the absorbing Mn, $R_{\mathrm{Mn–M}} = 2.82$ Å, in the second coordination sphere. The comparison between the computed and the experimental spectra shown in figure 1(a) reflects the structural origin of the main spectral resonances (A to F). Indeed, the computation obtained by using the small cluster does not correctly reproduce the relative energy separation between features A and B in the near-edge region or the shape of the broad resonance (F) in the high-energy region. As further coordination shells, and thus both single and multiple-scattering contributions within the first 4.5 and 6 Å around Mn, are added to the computation the agreement between the theoretical and the experimental spectrum improves regarding both the shape and energy position of the different spectral features. As shown in figure 1(b), no differences are found between computations performed for clusters including contributions from atoms located within the first 7 and 7.5 Å around the photoabsorber. This result indicates that the excited photoelectron probes an atomic cluster of about 7 Å around the absorbing Mn site during its lifetime and, consequently, further coordination shells do not contribute significantly to the XANES spectrum.

Once the cluster size has been fixed we have tested the performance of different exchange and correlation potentials (ECP) to account for the experimental spectrum. In this way, as shown in panels (b) and (c) of figure 1, we have computed the Mn K-edge XANES of Mn_3SnC by using the real X_α and the complex (energy dependent) HL ECP potentials. For the sake of completeness we have also performed the calculation by taking only the real part of the HL potential. In addition, the same computation has been performed by using the energy-dependent DH exchange potential and by adding to it the imaginary part of the HL ECP. All the calculated theoretical spectra have been further convoluted with a Lorentzian shape function with $\Gamma = 1.5$ eV.

As shown in figure 1, the computations reproduce all the spectral features fairly well, with the exception of the broad D peak. As expected, the use of complex potentials leads to a significant improvement in the intensity ratio between the different spectral features because the imaginary part of the HL potential accounts for the inelastic losses of the photoelectron [15]. The best reproduction of the experimental XANES spectrum is obtained by using the DH exchange and the imaginary part of the HL ECP (hereafter the *complex* Dirac–Hara).

The same class of computations has been performed for both Mn_3ZnC and Mn_3GaC cases. As shown in figure 2 the agreement between the *ab initio* calculations and the experimental data is remarkable. However, it should be noted that despite the main spectral features being accounted for by the calculations, the same does not hold for the shape of the XANES spectrum in the region between the main peak (C) and the broad resonance (D). Indeed, going from Sn to Ga the absorption increases in such a way that for Mn_3GaC a new structure, C_1, is clearly observed. A similar structure is also present in the case of Mn_3ZnC, although its intensity is rather weak. In contrast to the experimental results, the computations do not show any trace of this emerging structure.

The intensity of the C_1 peak increases as the interatomic distance between the absorbing Mn and the nearest C atoms decreases. We ask ourselves whether this finding is related

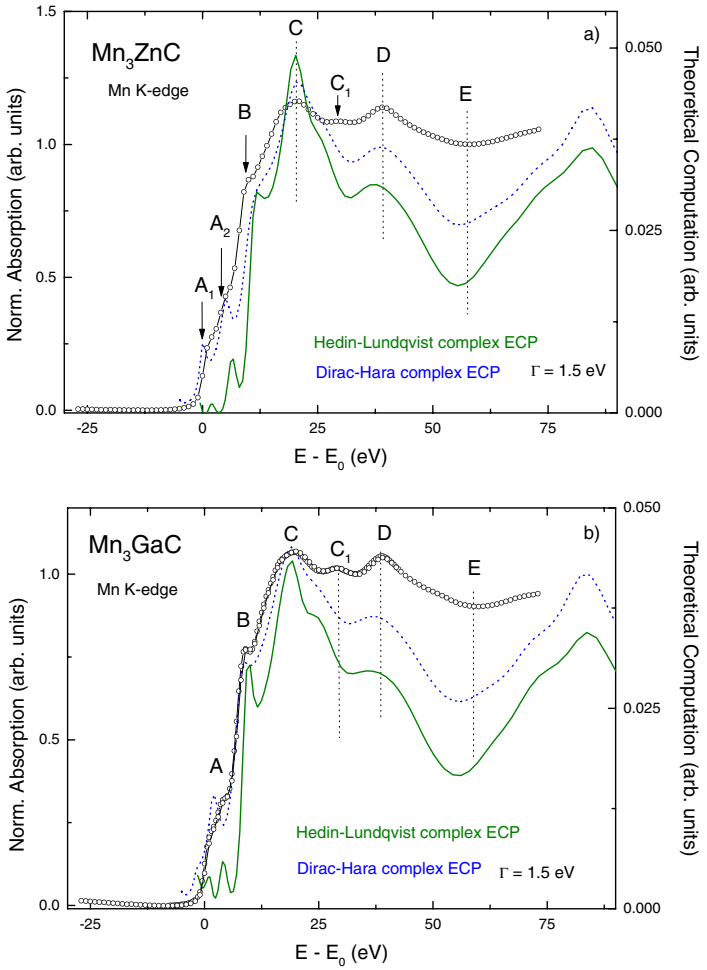

Figure 2. Comparison of the experimental Mn K-edge XANES spectrum (O)and the result of the *ab initio* calculations performed for a 7 Å cluster and by using the Hedin–Lundqvist (green, solid) and the complex (see text for details) Dirac–Hara (blue, dots) ECP potentials in the case of (a) Mn_3ZnC and (b) Mn_3GaC.

to the electronic transfer between Mn and C that should be favoured as the interatomic distance decreases. To verify this possibility we have performed a self-consistency field (SCF) procedure in order to obtain both (i) a more realistic charge density than for the neutral atom approximation, and (ii) its perturbation by the creation of the core-hole during the ionization process. Due to the impossibility of building SCF potentials for clusters with a large number of atoms, we have stabilized a small neutral MnC_2 cluster by considering a Mn^{2+} electronic state. Then, this cluster has been embedded into the larger, 7 Å, one to perform the multiple-scattering calculations for a cluster containing 107 atoms. Within this approximation the potential of both the absorbing Mn and of the two nearest-neighbours C atoms is SCF, while the potential around other atoms was built according to the Mattheis' prescription. This procedure has been previously shown to be successful on extended systems [22–26].

Results of the calculations performed for both HL and DH ECP potentials are reported in figure 3. It is noticeable that the use of the SCF potential yields a spectral profile closer to

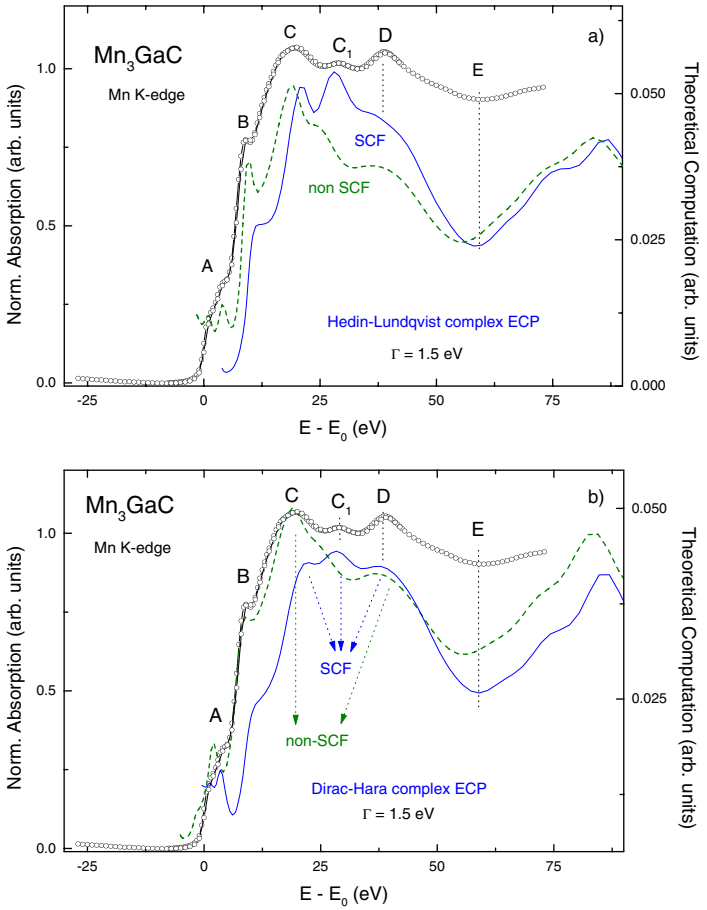

Figure 3. Comparison of the experimental Mn K-edge XANES spectrum of Mn_3GaC (○) and the result of the *ab initio* calculations performed for by using SCF (blue, solid line) and non-SCF (green, dashed line) potentials: (a) Hedin–Lundqvist ECP; (b) Dirac–Hara ECP.

the experimental one, whatever the ECP (HL or DH) considered. The previously missing C_1 feature is clearly reproduced by the computations. This result points out the special nature of the Mn–C bonding within the metallic frame. The SCF computations accurately reproduce the high-energy region of the XANES by accounting for all the spectral features experimentally observed, their relative intensity as well as their energy position. However, it should be noted that despite the above improvement in the agreement between the SCF computations and the experimental data, the reproduction of the near-edge region worsens. In particular, the main absorption peak C becomes narrower and there is also a shift of peak B towards higher energies. The comparison shown in figure 3 indicates the need to include a charge transfer between Mn and C atoms in order to reproduce the experiments. Indeed, the SCF calculation leads, by using the complex DH ECP potential, to the appearance of the missed C_1 structure and a better reproduction of the energy separation of the high-energy spectral features. However, it should be noted that our approach is to some extent rather crude. The SCF stabilized MnC_2 cluster involves the transfer of two electrons from Mn to C. However, in the real solid, C atoms are surrounded by six Mn atoms and the charge transferred from each Mn should be

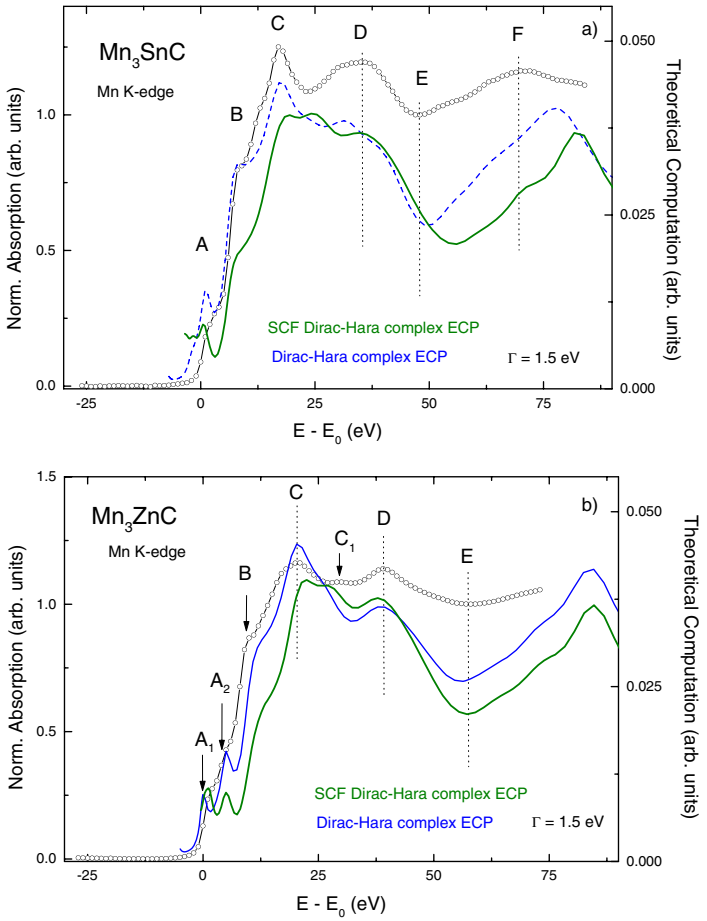

Figure 4. Comparison of the experimental Mn K-edge XANES spectrum (O) of Mn_3SnC (panel a) and Mn_3ZnC (panel b) and the result of the *ab initio* calculations performed using SCF (blue, solid line) and non-SCF (green, dashed line) Dirac–Hara ECP potentials.

fractional. Unfortunately, the SCF procedure of the CONTINUUM code is not able to handle this fractional charge transfer.

Finally, we have applied the same SCF procedure to the case of both Mn_3ZnC and Mn_3SnC. As shown in figure 4 also in these cases the use of the SCF potential leads to the appearance of a new structure in between the main C and D spectral features. Therefore, we conclude that the presence of such a C_1 peak on the experimental spectrum is a fingerprint of the charge transfer between Mn and C atoms and that this transfer is favoured as the Mn–C interatomic distance decreases. Indeed, in the case of Mn_3SnC showing the longest Mn–C distance, the C_1 peak is absent in the experimental XANES spectrum and it can be reproduced by using charge densities of neutral atoms. The case of Mn_3ZnC is intermediate between those of Ga and Sn compounds. The C_1 feature is present on the spectrum but its intensity is depressed. Hence, in this case as well it is necessary to consider both SCF and non-SCF potentials to account for the experimental shape. We therefore note that the position of the absorption minimum E at ∼48 eV above the edge is an indicator of the need to include charge transfer. In the case of Mn_3SnC, the standard computation performed by using charge

densities for neutral atoms perfectly accounts for the energy difference between peak C and the minimum E. By contrast, the position of the minimum is shifted to higher energy in the SCF calculation in disagreement with the experimental behaviour. However, in those cases in which the appearance of the C_1 feature indicates the need to include the charge transfer, the SCF computation yields the right energy separation between those C and E spectral features.

4. Summary and conclusions

We have presented the detailed *ab initio* computation of the Mn K-edge XANES spectra in the case of Mn_3SnC, Mn_3ZnC and Mn_3GaC compounds performed within the multiple-scattering framework.

Comparison of the experimental Mn K-edge XANES spectra of the three Mn_3MC compounds reveals the appearance of an additional spectral feature whose intensity is enhanced as the distance between Mn and its nearest-neighbours C atoms decreases. Our calculations have shown that this feature is not related to any structural modification. On the contrary, they identify it as being due to charge transfer between Mn and C atoms. The presence of such a structure is well reproduced by calculations performed using SCF potentials for the photoabsorbing Mn and its two next-neighbouring C atoms accounting for such an electron transfer.

These results point out the special nature of the Mn–C bonding in these systems, in agreement with recent theoretical calculations [27]. While the Mn–C charge transfer appears to be fundamental in the case of Mn_3GaC, its influence diminishes as the Mn–C distance increases in such a way that it has no influence in the case of Mn_3SnC. Comparison of experimental data and our *ab initio* computations supports previous band structure results suggesting a critical role for the hybridization between Mn 3d and C 2p states in determining the magnetic properties of Mn_3MC systems.

Acknowledgments

This work was partially supported by the Spanish CICYT (grant MAT2005-06806-C04-04). This work was supported by the Japanese Society for the Promotion of Science: Invitation Fellowship Program for Research in Japan (short term). The synchrotron radiation experiments were performed at SPring-8 (proposals 200A0383-NS-np and 2003A0652-NS2-np).

References

[1] Fruchart D and Bertaut E F 1978 *J. Phys. Soc. Japan* **44** 781
[2] Kaneko T, Kanomata T and Shirakawa K 1987 *J. Phys. Soc. Japan* **56** 4047
[3] Fruchart D, Bertaut E F, Sayetat F, Nasr Eddine M, Fruchart R and Senateur J P 1970 *Solid State Commun.* **8** 91
[4] Fruchart D, Bertaut E F, Le Clerc B, Khoi L D, Veillet P, Lorthioir G, Fruchart E and Fruchart R 1973 *J. Solid State Chem.* **44** 781
[5] Kamishima K, Goto T, Nakagawa H, Minura N, Ohashi M, Mori N, Sasaki T and Kanomata T 2000 *Phys. Rev.* B **63** 024426
[6] Kim W S, Chi E O, Kim J C, Choi H S and N H Hur 2001 *Solid State Commun.* **119** 507
[7] Jardin J P and Labbe' J 1983 *J. Solid State Chem.* **46** 275
[8] Motizuki K and Nagai H 1988 *J. Phys. C: Solid State Phys.* **21** 5251
[9] Shim J H, Kwon S K and Min B I 2002 *Phys. Rev.* B **66** 020406(R)
[10] Uemoto S, Maruyama H, Kawamura N, Uemura S, Kitamoto N, Nakao H, Hara S, Suzuki M, Fruchart D and Yamazaki H 2001 *J. Synchrotron Radiat.* **8** 449
[11] Takahashi M and Igarashi J 2006 *Phys. Rev.* B **67** 245104

[12] Natoli C R and Benfatto M, unpublished
Benfatto M, Natoli C R, Bianconi A, García J, Marcelli A, Fanfoni M and Davoli I 1986 *Phys. Rev.* B **34** 5774
[13] Natoli C R and Benfatto M 1986 *J. Physique* **47** C8–11
[14] Lee P A and Pendry J B 1975 *Phys. Rev.* B **11** 2795
[15] Natoli C R, Benfatto M, Della Longa S and Hatada K 2003 *J. Synchrotron Radiat.* **10** 26
[16] See for example Chaboy J and Quartieri S 1995 *Phys. Rev.* B **52** 6349 and references therein
[17] Mattheis L F 1964 *Phys. Rev.* A **133** 1399
Mattheis L F 1964 *Phys. Rev.* A **134** 970
[18] Norman J G 1974 *Mol. Phys.* **81** 1191
[19] Clementi E and Roetti C 1974 *At. Data Nucl. Data Tables* **14** 177
[20] Lee P A and Beni G 1977 *Phys. Rev.* B **15** 2862
[21] Krause M O and Oliver J H 1979 *J. Phys. Chem. Ref. Data* **8** 329
[22] Chaboy J, Muñoz-Páez A and Sánchez Marcos E 2006 *J. Synchrotron. Radiat.* **13** 471
[23] Chaboy J, Muñoz-Páez A, Carrera F, Merkling P J and Sánchez Marcos E 2005 *Phys. Rev.* B **71** 134208
[24] Chaboy J, Muñoz-Páez A, Merkling P J and Sánchez Marcos E 2006 *J. Chem. Phys.* **124** 064509
[25] Wu Z Y, Benfatto M and Natoli C R 1992 *Phys. Rev.* B **45** 531
[26] Pedio M, Benfatto M, Aminpirooz S and Haase J 1994 *Phys. Rev.* B **50** 6596
[27] Kim I G, Jin Y J, Lee J I and Freeman A J 2003 *Phys. Rev.* B **67** 060407(R)